M 2015

U.PORTO
FEUP FACULDADE DE ENGENHARIA
UNIVERSIDADE DO PORTO

MULTI-EULERIAN CFD MODELING AND SIMULATION OF PILOT-SCALE EBULLATED-BEDS

JOANA FILIPA DOS SANTOS ROCHA

DISSERTAÇÃO DE MESTRADO APRESENTADA
À FACULDADE DE ENGENHARIA DA UNIVERSIDADE DO PORTO EM
ENGENHARIA QUÍMICA

Mestrado Integrado em Engenharia Química

Multi-Eulerian CFD modeling and simulation of pilot-scale ebullated-beds

Master Thesis

of

Joana Filipa dos Santos Rocha

Developed in the scope of the Dissertation course

carried out at

IFP Energies Nouvelles

Supervisor at FEUP: **Prof. José Carlos Lopes**

Supervisor at IFPEN: **Dr. Cláudio Fonte**

Dra. Vânia Santos-Moreau

Departamento de Engenharia Química

July of 2015

Declaration of Authorship

I solemnly declare that this work is original and that no part of it is taken from others without giving them the deserved credit. All sources were accordingly referenced in the work.

Porto, July 31, 2015

(Joana Filipa dos Santos Rocha)

Acknowledgements

Here I wish to thank Dr. Dominique Humeau, director of the Process Experimentation division, and Dr. Hervé Cauffriez, department head of the Experimentation Intensification department, for the opportunity to make my internship in IFPen.

I also wish to thank my academic supervisor, Professor José Carlos Brito Lopes, for allowing me to carry out my master thesis at IFPen and for his support during my training period.

To my IFPen supervisor, Dr. Cláudio Fonte, I am deeply indebted for the strength and encouragement given all through the internship and even before, and for his invaluable help during the development of this project. Also, I am very thankful for all the advices to help me integrate in France, and for your kindness.

To Dr.ª Vânia Santos-Moreau, I wish to thank for the availability, new ideas and her vote of confidence.

I also wish to thank all of the people who embraced the three Portuguese as their own, because without you we would feel lost.

A special thank you for my boyfriend, Bruno Sousa, who accompanied me in this journey, with all the patience and love in the world. Without him, I wouldn't be able to endure all the stress. Thank you for being there.

I would also like to thank André Lopes for being the third musketeer in this new adventure, for all the laughs and for helping correct my thesis.

I wish to thank all my friends and colleagues that helped me and made my path brighter at FEUP. They made those five years unforgettable.

Finally, I wish to thank my family:

To my parents who were always proud and believed in me. My mother who let me follow my dreams, even if she wished me at home, and my father who wanted me to be independent and live the world.

To my aunts, uncles and grandfather for all the support, strength and love they given me all through my life.

To my cousins who made me want to be a better person and a role model for them.

Abstract

Many refining, pharmaceutical, food, and petrochemical industries have processes that involve chemical reactions between a liquid and a gas, supported on a solid catalyst, in an ebullated bed reactor. The lack of highly resolved non-invasive measuring techniques is part of the reason why these type of reactors have to rely on know-how to be properly designed. With the development of computational power, there were improvements in the field of Computational Fluid Dynamics (CFD) that allowed the understanding of complex interactions between the particle and fluid phases in fluidized beds. However, the modelling of these bed reactors is very challenging, as there are many interactions to be taken into account in the development of the model. For ebullated/fluidized beds there are two CFD approaches: the Lagrangian and the Eulerian approach.

In this work a Multi-Eulerian CFD approach is used to simulate both liquid and solid phases of an ebullated bed reactor with ANSYS® Fluent®.

The aims of this work are to choose appropriate parameters to simulate the ebullated bed reactor and to validate the model developed with data from the literature.

In the first part, the column height, the grid refinement, and the settings to the solid phase properties were studied for the ebullated bed reactor. In the second part, the Multi-Eulerian model was adapted to a similar case from the literature, and it was validated with experimental data.

Among all the simulations performed, the parameters which provided better results were the column with the length of 0.25 m, the grid with 540k elements, and second settings used to describe properties of the solid phase. For the validation of the model, the simulation using the Set 2 and a specularity coefficient of 1 to describe the interaction between the particles and the reactor wall provided results closer to experimental data.

Keywords: CFD simulation, ebullated beds, Multi-Eulerian

Resumo

Muitas refinarias e indústrias farmacêuticas, alimentares e petroquímicas têm processos em reatores de leito do tipo *ebullated*, que envolvem reações entre um líquido e um gás, num suporte sólido catalítico. Para fazer o projeto deste tipo de reatores, ainda é necessário basear-se no *know-how*, uma vez que existem poucas técnicas não-invasivas de alta resolução. Com o aumento do poder computacional, houve melhorias na área de Computational Fluid Dynamics (CFD), o que permitiu uma compreensão mais aprofundada das interações entre as particulas e a fase fluida em leitos fluidizados. No entanto, a modelização deste tipo de leitos é bastante exigente, visto que existem muitas interações a ter em conta no desenvolvimento do modelo. Em CFD, para leitos fluidizados e do tipo *ebullated* existem duas abordagens: a abordagem Lagrangeana e a Euleriana.

Neste trabalho é utilizado um método de CFD Multi-Euleriano para simular tanto a fase líquida como a fase sólida num reator de leito do tipo *ebullated* com o programa ANSYS® Fluent®.

Os objetivos deste trabalho são escolher os parâmetros apropriados para simular reatores de leito do tipo *ebullated* e validar o modelo desenvolvido com dados retirados da literatura.

Na primeira secção foi realizado um estudo à influência da altura do reator, do refinamento das grelhas e do conjunto de propriedades para a fase sólida num reator de leito do tipo *ebullated*. Na segunda secção, o modelo Multi-Euleriano foi adaptado a um caso semelhante da literatura e foi validado com dados experimentais.

Entre todas as simulações realizadas, os parâmetros com melhores resultados foram: a coluna com uma altura de 0.25 m, a grelha com 540k elementos e o segundo conjunto de propriedades (para descrever a fase sólida). Para a validação do modelo, a simulação em que os resultados estavam mais perto aos dos dados experimentais foi a que utilizou o Set 2 e um coeficiente de especularidade de 1 para descrever a interação entre as partículas e a parede do reator).

Table of Contents

List of Figures

List of Tables

Notation and Glossary

Ar	Arquimedes number	
C_D	Drag coefficient	
D	Column diamerter	m
d_p	Particle diameter	m
g	Gravitational acceleration vector	$m.s^{-2}$
H	Column length	m
K_{sl}	Coefficient of the momentum exchange between phases	$kg.m^{-3}.s^{-1}$
L	Bed height	m
p	Medium pressure	Pa
ΔP	Pressure drop	Pa
Re	Reynolds number	
t	Time	s
Δt	Time step	s
U	Inlet velocity	$m.s^{-1}$
U_{mf}	Minimum fluidization velocity	$m.s^{-1}$
U_t	Particle terminal velocity	$m.s^{-1}$
$\overline{u_k}$	Local time averaged velocity	$m.s^{-1}$
V_{li}	Solids terminal velocity	$m.s^{-1}$
v_l	Liquid velocity	$m.s^{-1}$
v'_k	Instantaneous local velocity	$m.s^{-1}$
v_s	Solids velocity	$m.s^{-1}$
Δx	Cell size	m

Greek letters

α	Volume fraction	
ε	Voidage	
λ_s	Granular bulk viscosity	$Kg.m^{-1}.s^{-1}$
μ	Fluid dynamic viscosity	Pa.s
ρ	Density	$Kg.m^{-3}$
τ	Viscous tensor	

Subscripts

i	
k	Phase indices
l	Liquid phase
s	Solid phase

List of abbreviations

2D	Two-dimensional
3D	Three-dimensional
CARPT	Computer aided radioactive particle tracking
CFD	Computational fluid dynamics
CT	Computer tomography
DEM	Dense element model
DPM	Dense particle model
FCCU	Fluid catalyst cracking unit
RMS	Root mean square
SC	Specularity coefficient
VOF	Volume of fluid

1 Introduction

Fluidized bed reactors are widely used in the chemical, pharmaceutical, petroleum, food and many other industries, and they have therefore been the focus of much research. This type of reactors are used in catalytic cracking, production of polymers, fluidized bed combustion, among other applications.

In spite of the industrial relevance of fluidized/ebullated bed reactors, proper design of commercial-size three-phase fluidized beds continues to rely on know-how. Part of the poor understanding comes from the lack of highly resolved measuring techniques that are capable of probing the inner reactor flow structure, and, at the same time, not disturb the solids' behavior to provide the refined experimental information needed for validation of general models based on basic principles.

Recent works have been reported intending to characterize the solids motions in gas-liquid-solid fluidized beds, while using advanced non-invasive measuring techniques, such as Particle Image Velocimetry (Chen *et al.*, 1994; Chaouki *et al.*, 1997) and radioactive particle tracking (Larachi *et al.*, 1996).

On the other hand, in recent years, with the significant development in computational power, Computational Fluid Dynamics (CFD) has become a viable tool for understanding the complex interaction between fluid and particle phases in fluidized beds. (Kiared *et al.*, 1997), (Cornelissen *et al.* 2007), and (Dadashi *et al.*, 2014) are examples for such improvements in the field. CFD enables researchers to do non-invasive multi-phase simulations with complex 3D geometries.

However, the modeling of fluidized/ebullated bed reactors is a quite challenging task. This is mainly due to their complex flow behavior and the many interactions (between the particles, between the particles and the fluids, and between the particles and reactor walls) to take into account in the model.

Different CFD approaches are employed for various reactors, but in general, two different categories are used for fluidized beds. One is the Lagrangian approach that takes into consideration particle-particle collision and forces acting on the particle while solving the equations of motion for each particle. The second is the Eulerian approach that solves continuity and momentum conservation equations considering a interpenetrating continua the phases.

In this work a Multi-Eulerian CFD approach has been used to simulate both liquid and solid phases of an ebullated bed reactor with ANSYS® Fluent®.

1.1 Introduction to the Organization

IFP Energies Nouvelles (IFPEN) is a public research and training facility. It has an international scope, covering the fields of energy, transport and the environment. From research to industry, technological innovation is central to all its activities.

As part of the public-interest mission with which it has been tasked by the public authorities, IFPEN focuses on:

- providing solutions to take up the challenges facing society in terms of energy and the climate, promoting the emergence of a sustainable energy mix;
- creating wealth and jobs by supporting French and European economic activity, and the competitiveness of related industrial sectors.

Its programs are hinged around 5 complementary, inextricably-linked strategic priorities:

- **renewable energies**: producing fuels, chemical intermediates and energy from renewable sources,
- **eco-friendly production**: producing energy while mitigating the environmental footprint,
- **innovative transport**: developing fuel-efficient, environmentally-friendly transport,
- **eco-efficient processes**: producing environmentally-friendly fuels and chemical intermediates from fossil resources,
- **sustainable resources**: providing environmentally-friendly technologies and pushing back the current boundaries of oil and gas reserves.

An integral part of IFPEN, its graduate engineering school prepares future generations to take up these challenges.

1.2 Contributions and Objective of the Project

The present work provides detailed information on a liquid/solid ebullated bed reactor using an Euler-Euler approach. Generally, in the literature the focus falls on the bubbling beds (gas/solid fluidization), therefore there is little information on liquid/solid beds. More so, the previous studies in this subject lack vital information to develop to more complex cases.

The main objective of this work was to develop and validate a simplified multi-Eulerian model for predicting the flow, volume fraction of solids and velocity fields. In addition, preliminary studies were made to set the column height, the grid refinement, and the solid phase properties, for future projects.

1.3 Thesis Structure

- This thesis is divided in 6 sections:Section 1, the present chapter, is the introduction and includes the context and the objectives of the work performed.
- In section 2, the state of art on ebullated/fluidized bed reactors, on correlations for pressure drop and voidage, and on simulation and respective models is addressed.
- Section 3 describes the main characteristics of the ebullated bed reactor in study
- Section 4 focuses on the description of the computational model, along with boundary and initial conditions, and the used numerical methods.
- In section 5, the results for the preliminary studies and the validation of the Multi-Eulerian model with experimental data are provided.
- Finally on section 6 conclusions based on the attained results are drawn. Recommendations for future work are also included.

2 Context and State of the Art

With the ever increasing consumption and future predicted shortage of oil, there is the urge in the refining and petrochemical industries to optimize the existing technologies and develop new ones. One of those technologies is the ebullated bed reactors, which are used in hydrocraking of heavy petroleum fractions, and are key factors in sediments formation, catalyst attrition and catalyst deactivation.

In this section, a thorough description of ebullated bed reactors and a representative list of the current knowledge about numerical models to simulate ebullated/fluidized beds are presented, as well as theoretical and experimental correlations for parameters estimation.

2.1 Ebullated bed reactors

A fluidized bed is formed when a quantity of solid particles (normally held in a suitable vessel) are suspended by the forced introduction of an ascending fluid flow through the particulate medium. This medium starts to fluidize when the forces applied on the particles are greater than its weight. This phenomena, called fluidization, causes the solid/fluid mixture to behave like a fluid, which results in the appearance of new characteristics that describe the medium, such as the ability to free-flow under gravity, or to be pumped using fluid type technologies (Zhu *et al.*, 2005). The pressurized fluid's presence reduces the mean density of the medium without affecting its fundamental nature.

There are different types of multi-phase reactors that work with this type of phenomena, like the trickle-bed reactor, slurry reactor, and ebullated bed reactor, which have diverse applications in catalytic reaction engineering.

In the present work, the ebullated-bed reactor is going to be studied. The inherent advantages of a good back-mixed bed are excellent temperature control and, since channeling and bed plugging are eliminated, a decrease in the constant pressure drops over several years of continuous usage. As a result, ebullated-bed reactors have the distinctive ability of stirred reactor type of operation with fluidized catalyst particles. Therefore, this kind of multi-phase reactor is most applicable for exothermic reactions and for reactions which are difficult to process in a fixed-bed or plug flow reactor. This difficulty is due to the accumulation of unwanted secondary products on the catalyst surface to the detriment of its function, designated as fouling. The ebullated-bed reactor is a fluidized-bed three-phasic system with an excellent continuous mixing between the liquid and the catalyst particles.

This type of reactors is widely used in the catalytic hydroconversion to improve heavy oils and petroleum residues that generally contain high concentration of heteroatoms, metals, and asphaltenes (Del Bianco *et al.*, 1994). The catalyst used for the ebullated bed is typically a 0.8 - 4 mm of diameter ductile material with nickel-molybdenum active metals and it can be spherical or cylindrical. The upward lift of liquid reactants (feed oil plus recycle) and gas (hydrogen feed and recycle) hold the catalyst in a fluidized state. The gas/liquid mixture enter in the reactor plenum and is distributed across the bed through a distributor and grid plate. The height of the ebullated catalyst bed is controlled by the rate of the liquid recycle flow. This liquid rate is adjusted by varying the speed of the ebullating pump (i.e., a canned centrifugal pump) which controls the flow of ebullating liquid obtained from the internal vapor/ liquid separator inside the reactor.

The ebullated regime operates with velocities of about twice the minimum fluidization velocity (U_{mf}), in which the bed height increases 20 to 30% from the initial value. This means that the particles are suspended however still within close distance from one another. Working in the ebullated regime, results in low reactor pressure drop, and a back-mixed and nearly isothermal bed. The introduction of fresh catalyst and the withdrawal of the old catalyst control the level of catalyst activity in the reactor. The ability of daily addition of a small catalyst quantity is a main feature of the ebullated-bed reactor and results in constant product quality over long time periods. To adjust operation for different feeds or levels of desired performance, the type of catalyst used can also be changed without stopping the reactor.

The run length of an ebullated bed is typically determined by other factors such as the inspection schedule of an entire processing facility. Because of this advantage, ebullated beds are well suited for applications requiring a long, continuous run length such as for pretreatment of FCCU (Fluid Catalytic Cracking Unit) feedstocks (typically 3 years) (Kressmann *et al.*, 2000).

2.1.1 Correlations for pressure drop

Over the last century, several theoretical and experimental correlations have been proposed to describe the influence of pressure drop (ΔP in Pa) in biphasic packed and fluidized beds. One of the more well-known is the Ergun equation (Ergun, 1952), an empirically-derived equation that relates the pressure drop in a packed bed with the viscous and inertial loss. This equation describes the pressure drop variation until the inlet velocity (U in m.s^{-1}) reaches the minimum fluidization velocity. From this velocity onwards, the fluidized bed pressure stays in equilibrium, and the beds height (L in m) starts increasing.

$$\frac{\Delta P}{L} = 150\frac{(1-\varepsilon)^2}{\varepsilon^3}\mu\frac{U}{d_p^2} + 1.75\frac{1-\varepsilon}{\varepsilon^3}\rho\frac{U^2}{d_p} \qquad \textit{Eq. 1}$$

where μ (Pa.s) is the viscosity of the fluid, d_p (m) is the particle diameter, and ρ (kg.m^{-3}) is the liquid density.

$$\frac{\Delta P}{L} = (\rho_s - \rho)\vec{g}(1-\varepsilon) \qquad \textit{Eq. 2}$$

where ρ_s (kg.m^{-3}) is the solids density and $\vec{g}$ (m.s^{-2}) is the gravity acceleration. Eq. 2 is derived from the consideration made for a suspended particle, where the particle weight ($\vec{P}$) is equal to the impulsion ($\vec{I}$) induced by the fluid to the particle ($\vec{P} - \vec{I} = \vec{0}$). The minimum fluidization velocity (U_{mf}) is obtained from Eq. 3, which is derived from the consideration that, in the minimum fluidization point, ΔP in both Eq. 1 and Eq. 2 are the same.

$$Ar = 150\frac{1-\varepsilon}{\varepsilon^3}Re_{mf} + 1.75\frac{1}{\varepsilon^3}{Re_{mf}}^2 \qquad \textit{Eq. 3}$$

where the Arquimedes number (Ar) is determined by $Ar = \frac{\rho(\rho_s-\rho)\vec{g}d_p^3}{\mu^2}$ and the Reynolds number at the minimum fluidization point is $Re_{mf} = \frac{\rho U_{mf} d_p}{\mu}$.

Another empirical correlation, also known worldwide, is the Richardson-Zaki correlation (Richardson and Zaki, 1954). This equation relates the dependency of the inlet velocity on the voidage fraction (ε), for velocities higher than the minimum fluidization velocity.

$$U = U_t \varepsilon^n \qquad \textit{Eq. 4}$$

where U_t (m.s^{-1}) is the terminal settling velocity of a single particle, and the parameter n, listed in Table 1, is a function of the flow regime and the particle to column diameter ratio.

Table 1. Values of the parameter n by Richardson and Zaki (1954).

$Re_t < 0.2$	$n = 4.65 + 19.5\, d_p/D$
$0.2 < Re_t < 1$	$n = (4.35 + 17.5\, d_p/D){Re_t}^{-0.03}$
$1 < Re_t < 200$	$n = (4.45 + 18\, d_p/D){Re_t}^{-0.1}$
$200 < Re_t < 500$	$n = 4.45{Re_t}^{-0.1}$
$Re_t > 500$	$n = 2.39$

where $Re_t = \frac{\rho U_t d_p}{\mu}$ is dimensionless and corresponds to the particle Reynolds number at the terminal velocity.

Limtrakul *et al.* (2005) modified the Richardson-Zaki equation to better predict the bed voidage fraction.

$$U = V_{li} \varepsilon^n \qquad \textit{Eq. 5}$$

where $\log V_{li} = \log U_t - d_p/D$, and d_p and D are the particle and column diameter, respectively. The parameter n in Eq. 5 can be attained from the correlation proposed by (Garside et Al-Dibouni 1977) set by Eq. 6:

$$n = \frac{5.09 + 0.284 Re_t^{0.877}}{1 + 0.104 Re_t^{0.877}} \qquad \textit{Eq. 6}$$

2.2 Simulation of ebullated/fluidized beds

The development of CFD techniques is used to solve conservation and momentum equations in multiphase flows. This technique is an advanced research area for envisioning major phenomena without carrying real-time experiments. In case of a fluidized bed reactor, CFD gives the advantage of describing phase interactions, particle/wall interactions and preferred flow paths for the liquid and/or gas. It also allows access in every phase and in all of the dominium to all variables. CFD simulations have the advantage of studying a high number of operation conditions and geometries without having to build prototypes, which have operation and construction costs associated. A notorious drawback of the CFD modeling of a multiphasic reactor is its long computational time, but when faced with its benefits, it's a safe choice when experimenting with different materials, inlet velocities, geometries, among others.

When required to describe liquid-solid and gas-solid fluidized reactors, two forms of CFD approaches are generally used, i.e., Eulerian and Lagrangian approaches. In this section, the different approaches and respective models available in Fluent® are going to be described.

2.2.1 Eulerian-Eulerian approach

The Euler-Euler approach was developed for modeling two or more phases, treating them as interpenetrating continua. This approach solves momentum and continuity equations for multi-phase flow. Since the volume of a phase cannot be occupied by the volume of other phases, the volume fraction concept is introduced and can be obtained, like the phase's mean velocities, by the equations mentioned. There are various models using this approach, like the Eulerian model, Mixture model, and volume of fluid (VOF) model.

- The Eulerian model

The Eulerian model is the most complex of the multiphasic models as it solves a set of n momentum and continuity equations. Coupling is achieved through the pressure and interphase exchange coefficients. This model is computationally cost effective and also suitable to cases where body forces, like gravity, have a major interaction within and between phases. This method covers fluidized/ebullated beds, risers, bubble columns and

particle suspensions, and it's only limited by hardware memory constraints and convergence issues.

- The mixture model

The mixture model is simpler than the Eulerian model, as it solves a smaller number of equations. This model solves the mixture momentum equation and assesses relative velocities to describe the dispersed phases. Sedimentation, bubbly flow, particle-laden flow with low loading and cyclone separator are examples of the mixture model applications. The mixture model can also be used without relative velocities for the dispersed phase to model homogeneous multiphase flows.

- The VOF model

The VOF (volume of fluid method) approach is a surface-tracking technique applied to a fixed Eulerian mesh and is designed to model multiple immiscible fluids. Examples of this model applications include motion of fluid through a system, calculation of motion of large bubbles in a liquid, jet breakup and steady or transient movement of the multi-fluidic interface. However, the VOF model has also some limitations, like the requirement of all control volumes being filled with either a single fluid or a combination of phases. This model doesn't allow void regions where no fluid is present, and only a single phase can be described as a compressible ideal gas. The VOF model also cannot be used with the discrete particle model (DPM) for gas–solid reaction modeling in which particles are analyzed in parallel.

2.2.2 The Eulerian-Lagrangian approach

In this model, the equations of motions (Newton's Second Law) are solved for every particle in the medium and it takes into account the particle-particle collisions and other forces acting on the particle. This approach is also recognized as DPM or discrete element model (DEM) and it uses the Eulerian framework to model the fluid phase, considering it as a continuum phase, while the trajectories of the particles are simulated in the Lagrangian framework, where the solids are considered as a dispersed phase.

3 Studied System

The studied reactor is used for testing catalysts used in conversion and hydroconversion of heavy crude oil products to diesel. It consists of cylindrical reactor, which has a cylindrical catalytic metal basket and propeller. The catalytic basket is closed in the bottom and top with a perforated grid, and it is used to support the catalyst particles and to avoid their contact with the propeller. The sidewalls of the basket are solid and impermeable to the passage of fluids, while the top and bottom grids have an appropriate size to allow the passage of gas/liquid through the catalyst and, thus, put it in suspension. The axial turbine from the stirring system conveys the mixture transportation from the bottom up through the basket. The reagents (hydrocarbons and hydrogen) enter the reactor through the bottom, whereas the (gas and liquid) products exit from the top, as it is shown in Figure 1.

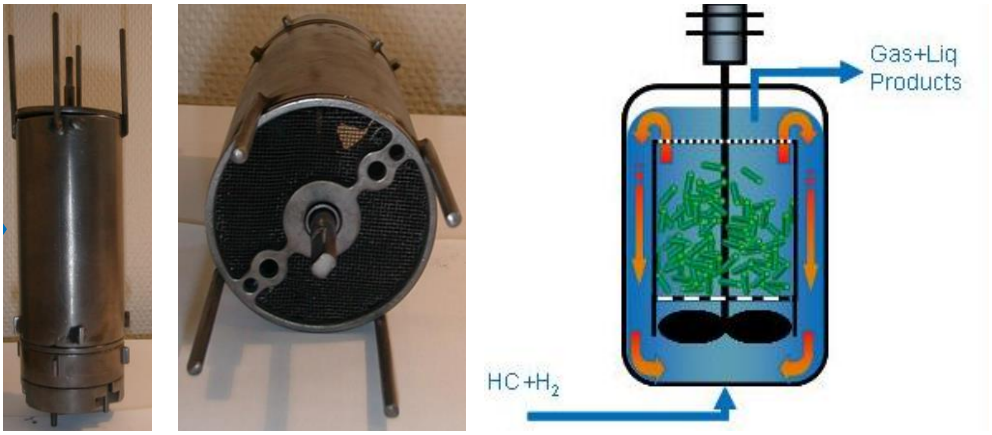

Figure 1. Reactor carcass and basket (in the left) and a schematic diagram of the ebullated bed reactor in study (on the right).

The volume of the reactor is of 1 L, with 0.08 m of diameter and 0.240 m of height. The reactor basket has a diameter of 0.063 m and is 0.120 m high. The cylindrical particles have a diameter of 1 mm and have between 3 to 5 mm of length.

The simulation of this kind of multi-phasic reactors with non-spherical catalyst particles is not an easy task, and there are no previous works in the literature in this field of ebullated bed simulation. A simplified CFD model has been developed as a first approach to start studying the system. The proposed simplifications were considered according to the available data found in the literature to validate the model. The assumed simplifications are:

- The reactor is two-phasic instead of a three-phasic one, neglecting for the moment the presence of gas.
- The catalyst particles are spherical instead of cylindrical, avoiding the need to introduce the sphericity in the simulation.

- The flow of the liquid in the inlet is uniform and purely ascending, meaning that the effect of velocity profile at the inlet generated by the propeller is not considered.

The ultimate objective of this thesis is to be used as a foundation to completely simulate the studied reactor. However, to validate the model, experimental data for a similar case in the literature was necessary as it was inexistent for the pilot-scale reactor with the previous considerations.

Limtrakul *et al.* (2005) used non-invasive gamma rays-based techniques, computer tomography (CT) and computer aided radioactive particle tracking (CARPT) to measure solid holdup and solid velocity contours in liquid/solid fluidized beds, respectively. This study has the motivation of being used to validate CFD models.

studied two different columns, one with 0.10 m internal diameter and 2 m height and the other with 0.14 m internal diameter and 1.5 m height. Both columns have similar configurations and measurements to the pilot-scale reactor in study. The fluid is tap water, and the solids are either glass or acetate beads. The glass beads have 0.001 m ($\rho_s = 2900$ kg/m^3) or 0.003 m in diameter ($\rho_s = 2500$ kg/m^3) and the acetate beads have a diameter of 0.003 m ($\rho_s = 1300$ kg/m^3).

4 Computational Model Description

4.1 Geometrical domain and discretization

For an impartial comparison of CFD model with experimental data, it is important to execute simple fluidization experiments where all the parameters, like the mesh refinement, the solid phase properties, the drag model, among others, are as well characterized as possible. Even though the validation of the CFD model is necessary, this work will start with the study of the ebullated-bed reactor basket, shown in Figure 2 as a schematic diagram. The column has a height of 0.25 m and a diameter of 0.10 m, the spherical catalyst particles have 0.003 m of diameter ($\rho_s = 2500$ kg/m^3) and the bed height is of 0.05 m. The fluid passing through the column is water and the inlet has an ascending flow. The voidage fraction present in the bed is 0.4.

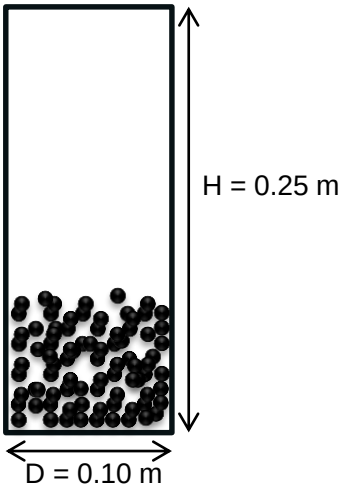

Figure 2. Schematic overview of an ebullated bed reactor.

The randomness of the catalyst particles, caused by preferred paths by the fluid in the bed changing in the transient flow, brings more complexity to the problem. As the particles in the ebullated bed collide with each other in every direction, a 3D geometric model is chosen, instead of a 2D geometric one, to describe the fluidization. This geometric model will convey a more realistic approach to compare with the literature experimental data.

Pressure drop in the medium was computed with area averaged values in the inlet and monitored during the simulation in order to compare with Eq. 1, Eq. 4, and Eq. 5, along with the bed height.

4.2 Governing Equations

The CFD model for the ebullated bed reactor is based on the Euler-Euler approach. Thus, the governing equations for both the solid and liquid phases have the same structure. The continuity equation for the phase i ($= l$ for liquid/$= s$ for solid) are given as:

$$\frac{\partial}{\partial t}(\alpha_i \rho_i) + \nabla.(\alpha_i \rho_i \overrightarrow{v_i}) = 0 \qquad \textit{Eq. 7}$$

where α_i is the volume fraction for phase i, ρ_i (kg/m^3) is the density and v_i (m.s^{-1}) is the velocity for phase i.

The momentum equation for the liquid phase is defined by:

$$\frac{\partial}{\partial t}(\alpha_l \rho_l) + \nabla.\left(\alpha_l \rho_l \overrightarrow{v_l}^2\right) = -\alpha_l \nabla p + \nabla.\overline{\overline{\tau_l}} + \alpha_l \rho_l \vec{g} + K_{sl}(\overrightarrow{v_s} - \overrightarrow{v_l}) \qquad \textit{Eq. 8}$$

$$\overline{\overline{\tau_l}} = \alpha_l \mu_l (\nabla.\overrightarrow{v_l} + \nabla.\overrightarrow{v_l}^T) \qquad \textit{Eq. 9}$$

where p is the medium's pressure, τ_l is the viscous stress tensor, $\vec{g}$ is the gravity acceleration and K_{sl} is the coefficient of the momentum exchange between the two phases. The momentum equation for the solids phase is given by:

$$\frac{\partial}{\partial t}(\alpha_s \rho_s) + \nabla.\left(\alpha_s \rho_s \overrightarrow{v_s}^2\right) = -\alpha_s \nabla p + \nabla p_s + \nabla.\overline{\overline{\tau_s}} + \alpha_s \rho_s \vec{g} + K_{ls}(\overrightarrow{v_l} - \overrightarrow{v_s}) \qquad \textit{Eq. 10}$$

$$\overline{\overline{\tau_s}} = \alpha_s \mu_s \left(\nabla.\overrightarrow{v_s} + \nabla.\overrightarrow{v_s}^T\right) + \alpha_s \left(\lambda_s - \frac{2}{3}\mu_s\right) \nabla.\overrightarrow{v_s}\overline{\overline{I}} \qquad \textit{Eq. 11}$$

where p_s is the solids pressure and λ_s is the granular bulk viscosity and describes the resistance of an emulsion to compression or expansion. The coefficient of the momentum exchange between the liquid and solid phases (K_{sl}) is described by the empirical drag correlation of Gidaspow (*Eq. 12*).

$$K_{sl} = \begin{cases} \frac{3}{4} C_D \frac{\alpha_s \alpha_l \rho_l |\overrightarrow{v_s} - \overrightarrow{v_l}|}{d_s} \alpha_l^{-2.65} & \alpha_l > 0.8 \\ 150 \frac{\alpha_s (1-\alpha_l) \mu_l}{{d_s}^2} + 1.75 \frac{\alpha_s \rho_l |\overrightarrow{v_s} - \overrightarrow{v_l}|}{d_s} & \alpha_l \leq 0.8 \end{cases} \qquad \textit{Eq. 12}$$

where C_D is the drag coefficient and d_s (m) is the solids diameter.

The Gidaspow drag model is a combination of the Wen and Yu drag model and the Ergun equation (Gidaspow, 1994). The Wen and Yu drag model uses a correlation from the experimental data of Richardson and Zaki. This correlation is valid for a diluted bed when the internal forces are negligible, meaning that the viscous forces dominate the flow behavior. The Ergun equation is derived for a dense bed and relates the drag to the pressure drop through a porous media.

The Reynolds number calculated for the velocity studied for the ebullated bed, i.e. twice the minimum fluidization velocity, is 6500. The Re belongs to a transition regime flow, not laminar, but also not completely turbulent. So, through the bed, it was assumed a turbulence-free flow, not including the possibility of local regions of turbulence. According to (Cornelissen *et al.*, 2007), in general, accounting for time-average turbulent behavior and turbulent interactions between phases can make simulations predictions more realistic for beds at high Reynolds number. However, unless an appropriate turbulence model with the correct empirical constants is chosen, the model calculations may be less consistent with experimental data than considering a laminar flow regime.

4.3 Boundary and initial conditions

Figure 3 shows the three-dimensional liquid-solid ebullated bed used in the present numerical simulations. The ebullated bed has 0.10 m of diameter and 250 mm in height, as mentioned before. The computational parameters are listed in section 4.4. Initially, the bed porosity is 0.4 and the velocity of liquid in the inlet is set to 0.065 $m.s^{-1}$, which is twice the minimum value of the velocity required for fluidization. The liquid phase is only injected in the axial direction, assuming a uniform distribution for the phase components, and the inlet solids velocity is zero. At the outlet, the pressure is set constant and uniform, and equal to 1 atm. The no-slip condition is set at the walls, i.e., velocity at the walls is set to zero.

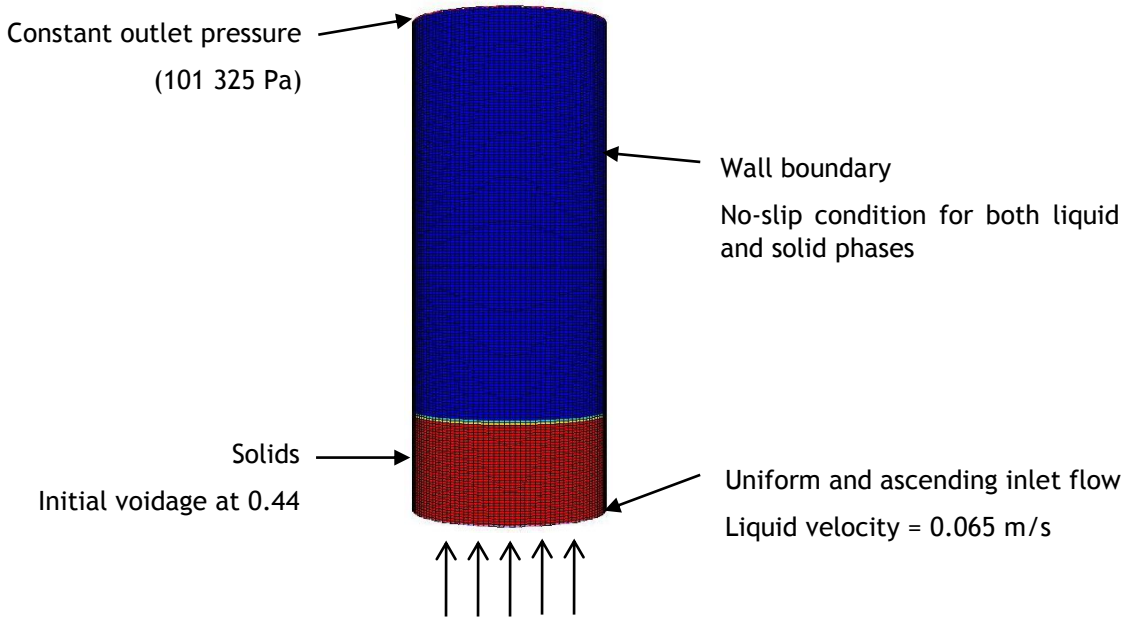

Figure 3. 3D geometric model and respective initial boundaries.

4.4 Model Parameters for the Solid Phase

When using an Eulerian model in Fluent®, it can be selected the granular model to solve the particulate medium. This model is described by several solid phase properties, which can be solved by different models. Some examples of the solid phase properties are the granular viscosity, the frictional viscosity, and the solids pressure. The granular viscosity methods specify the kinetic part of the granular viscosity of the particles; the frictional viscosity methods specify a shear viscosity based on the viscous-plastic flow and it is neglected by default, as shown in Set 1; and the solids pressure methods calculate its value to be used for the pressure gradient term in the solid-phase momentum equation *Eq. 10*.

The number of the solid phase properties varies with the multiphase model used and, occasionally, with the chosen method to solve a property. As such, the default settings for an Eulerian model have nine different properties, and without the sensibility to choose appropriate solving methods, it has more than 20 thousand possible combinations to test. In this case, the two sets of settings used were suggested by Ansys company:

- Set 1: obtained from the ANSYS Fluent Tutorial Guide: Using the Eulerian Granular Multiphase Model with Heat Transfer;
- Set 2: obtained from a training conference organized by Ansys.

Table 2. FLUENT settings for solid phase properties.

	Set 1 (Tutorial Ansys)	**Set 2 (Training Ansys)**	
Particle diameter	Constant: 0.003 m		
Granular viscosity	Syamlal-Obrien	Gidaspow	
Granular bulk viscosity	Lun et al.		
Frictional viscosity	None	Schaeffer	
		Angle of internal friction	Default Value
		Frictional pressure	Johnson et al.
		Frictional modulus	Derived
Granular temperature	Constant:1e-05	Constant: 0.55	
Solids pressure	Lun et al.	Algebraic	
Radial distribution	Lun et al.		
Elasticity modulus	Derived		
Packing limit	Constant: 0.6	Constant: 0.63	

4.5 Numerical Methods

DesignModeler and Meshing from the Ansys 15.0 suite, were used to create the ebullated bed geometry and to generate the computational mesh, respectively. The governing equations are solved by the CFD code ANSYS Fluent v15.0. A convergence criteria of 10^{-4} for each scaled residual, like velocities, continuity, and volume fraction, is used. The under-relaxation factors that are applied in the pressure-based solver to stabilize the convergence behavior of the external nonlinear iterations are listed in Table 3.

Table 3. Under relaxation factors

Pressure	0.5
Density	1
Body Forces	1
Momentum	0.2
Volume Fraction	0.5
Granular Temperature	0.2

The transient formulation is discretized by the second order upwind method, while the spatial discretization of the convection terms in the solution equations can controlled by several settings. The SIMPLE algorithm, using a segregated solution technique, is used to solve the pressure field and velocity field.

In Table 4 are listed the solution methods applied to the present work.

Table 4. Solution methods

Pressure-Velocity Coupling	Phase Coupled SIMPLE
Spatial Discretization	
Gradient	Least Squares Cell Based
Momentum	Second Order Upwind
Volume Fraction	First Order Upwind
Transient Formulation	Second Order Upwind

The Courant number (Eq. 13) is a necessary condition for convergence while solving partial differential equations. Essentially, it reflects the portion of a cell that a fluid will cross by advection in one time step. In this study, a constant Courant number, C, of 0.1 is used and a number maximum of 50 iterations per time step are considered.

$$C = U\frac{\Delta t}{\Delta x} \qquad \text{Eq. 13}$$

where U (m.s^{-1}) is the inlet velocity, Δt (s) is the constant time step and Δx (m) is the length of a mesh element.

5 Results and Discussion

This section presents two different studies: a parametric study and the validation of the model studied. The first is a preliminary study which analyses different parameters that may influence the ebullated bed reactor flow. In the second study, the model developed is applied to a different column to validate it using experimental data.

5.1 Preliminary studies

The objective of the preliminary studies is to understand how the model reacts to different parameters. In this parametric study, the overall bed voidage, and respective bed height, are predicted in the simulation. To study the system's dynamics, a surface and a line were created to follow the volume fraction of solids evolution and to follow the bed's height in the center of the column, respectively. Surface monitors were also created to follow the solids and liquid velocities in the x, y, and z directions.

In this parametric study, it was required to investigate the influence of the column height, mesh size, and proper sets of solid phase properties. Table 5 shows a list of the values considered in the preliminary studies.

Table 5. Base case settings and parametric studies studied.

Column Height	Mesh Size	Solid Phase Properties[1]
• 0.250 m	• 269k elements	• Set 1 (Ansys tutorial)
• 0.500 m	• 540k elements	• Set 2 (Ansys training)
	• 1 300k elements	

[1]The settings are shown in Table 2.

All the CFD simulations considered an inlet velocity of the liquid equal to twice the minimum fluidization velocity (U_{mf}), the outlet is at atmospheric pressure, and the velocities near the wall are considered zero (no-slip condition). The interaction between the particles and the liquid is described by the Gidaspow drag law, and a constant Courant number of 0.1 is used in the grid sensibility study.

5.1.1 Column height sensibility

Two columns with 0.25 and 0.5 m in height were used to assess the effect of column size. Both columns have 0.1 m in diameter, particles with 0.003 m of diameter, and a bed height of 0.05 m with a respective initial voidage of 0.4. To analyze the column height influence, less refined grids were considered, with $\Delta x = 2.5 \times 10^{-3}$ m. The higher column has twice the

number of elements of the smaller one and has 200 axial divisions, while the one with 0.25 m of length has 100.

In the CFD simulations, initial static bed was instantaneously fluidized with a uniform liquid velocity of 0.065 m/s at time 0 and maintained at this condition for 10 s. The overall bed voidage is plotted as function of time in Figure 4, along with the value obtained from the Ergun equation. The highest column is designated as $2H$ and the smallest as H, in the figure below.

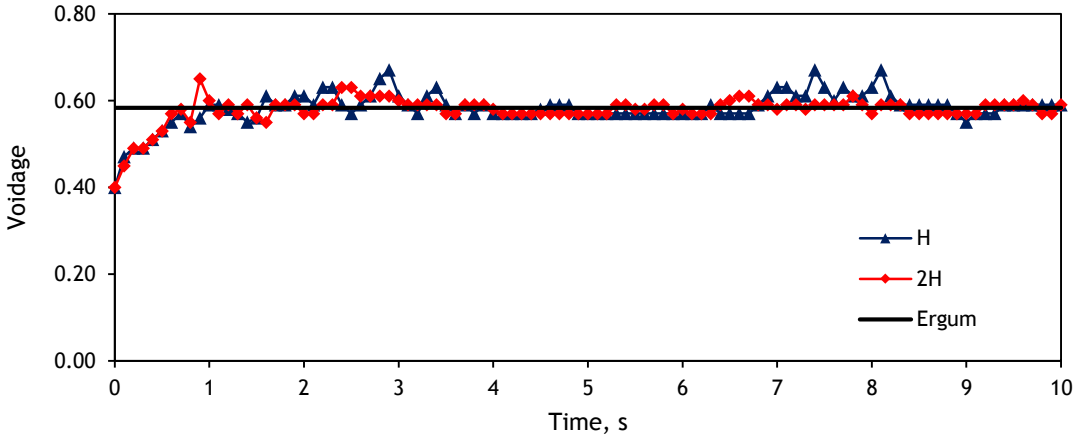

Figure 4. Effect of column height on overall voidage as a function of time. (H=0.250 m)

Considering only the overall voidage analysis, it is difficult to distinguish the behavior of the solids inside the columns. While the column with the height of 0.25 m (dark blue series – H) has small fluctuations in the voidage between 2 and 3.5 s and between 7 and 8.5 s, its behavior can be considered steady. As for the voidage as a function of time for the other column (red series – $2H$) stabilizes after 4 s of flow. Regardless, both overall voidage evolve around to the expected value of 0.58, obtained from the Ergun equation and the Richarson-Zaki correlation.

To further confirm that the column height does not influence significantly the behavior of the solids, the volume fraction of solids in a cut in the column at different times is analyzed. The Figure 5 shows the evolution of the solids flow in both columns at 0.4, 0.6, 1.2 and 10 s.

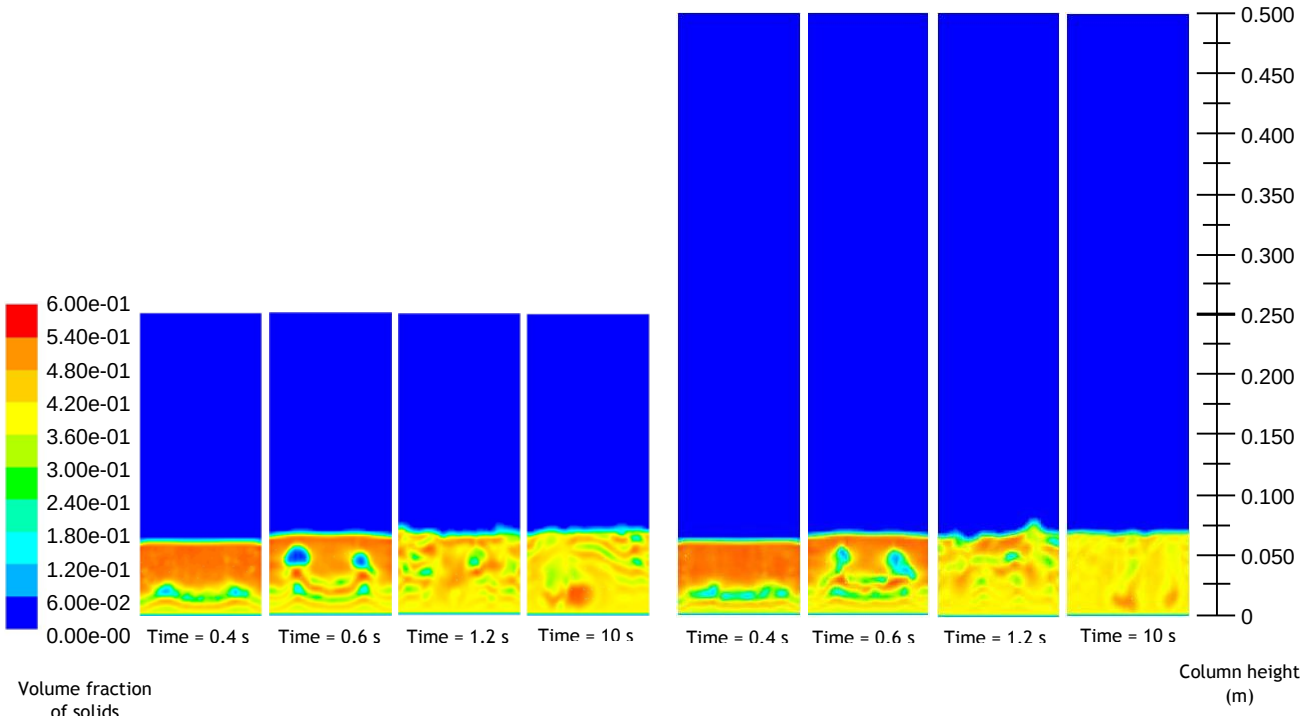

Figure 5. Dynamic sequence of the volume fraction of solids for the 0.250 m (left) and 0.500 m (right) columns at 0.4, 0.6, 1.2, and 10 s.

The solids movement displayed in the Figure 5 demonstrate a similar behavior, confirming what could be seen in Figure 4, that the column height does not influence to a great extent the results of the simulation. In further studies, the column of 0.250 m is selected, as it has less elements and therefore decreases the simulation time.

5.1.2 Grid sensibility

In this study, three different grids are going to be studied. The mesh with 270 000 elements has a $\Delta x = 2.5 \times 10^{-3}$ m and 100 divisions in the z direction; the mesh with 540 000 elements has a $\Delta x = 2.5 \times 10^{-3}$ m and 200 divisions in the z direction; and, finally, the mesh with 1 300 000 elements has a Δx and Δz of 1.5×10^{-3} m. As the particles have a diameter of 3 mm, all the cells dimensions have to be inferior to this value.

Whereas the first two grids have the same time step, since they have the same Δx, the last one has a bigger time step. The time steps are 3.84×10^{-3} and 2.31×10^{-3} s, respectively. All three grids had a maximum skewness factor (asymmetric probability distribution) of 0.35. To obtain this value for the finer mesh, it was necessary to divide the geometry in fours and only then was the sweep method applied. This method is included in the hexahedral category and requires consistent source and target faces. The sweep method can be readily used to maintain high solver accuracy at the same time as it reduces mesh cell counts (speeding solve times). The grids studied are shown in detail in Appendix 1.

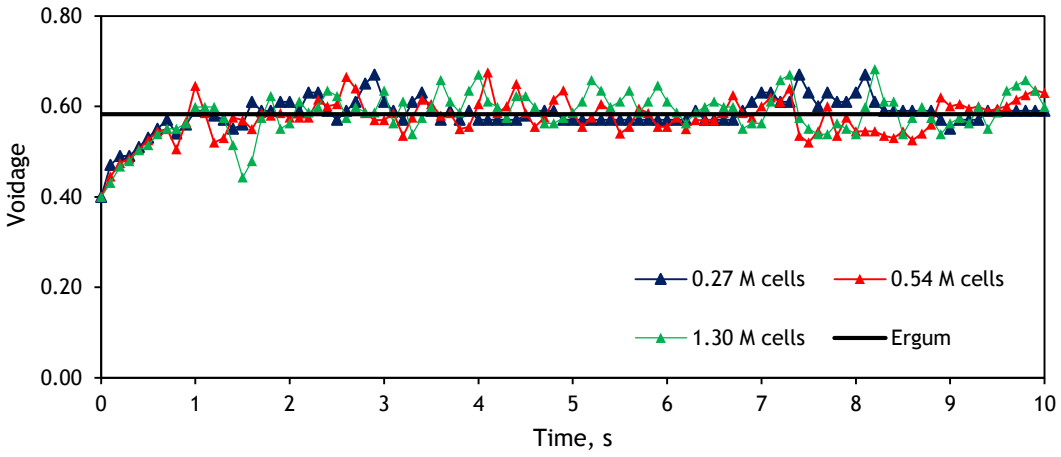

Figure 6. Effect of grid refinement on overall voidage as a function of time.

In the Figure 6 is shown the overall bed voidage as function of time plot with the value obtained from the Ergun equation. As it can be observed, the numerical simulations for all three mesh' resolutions are very similar. All three reach the voidage value of 0.58 (obtained from the Ergun equation) about 1 second after the increase in the inlet velocity and their behavior fluctuates around the value attained by the Ergun equation.

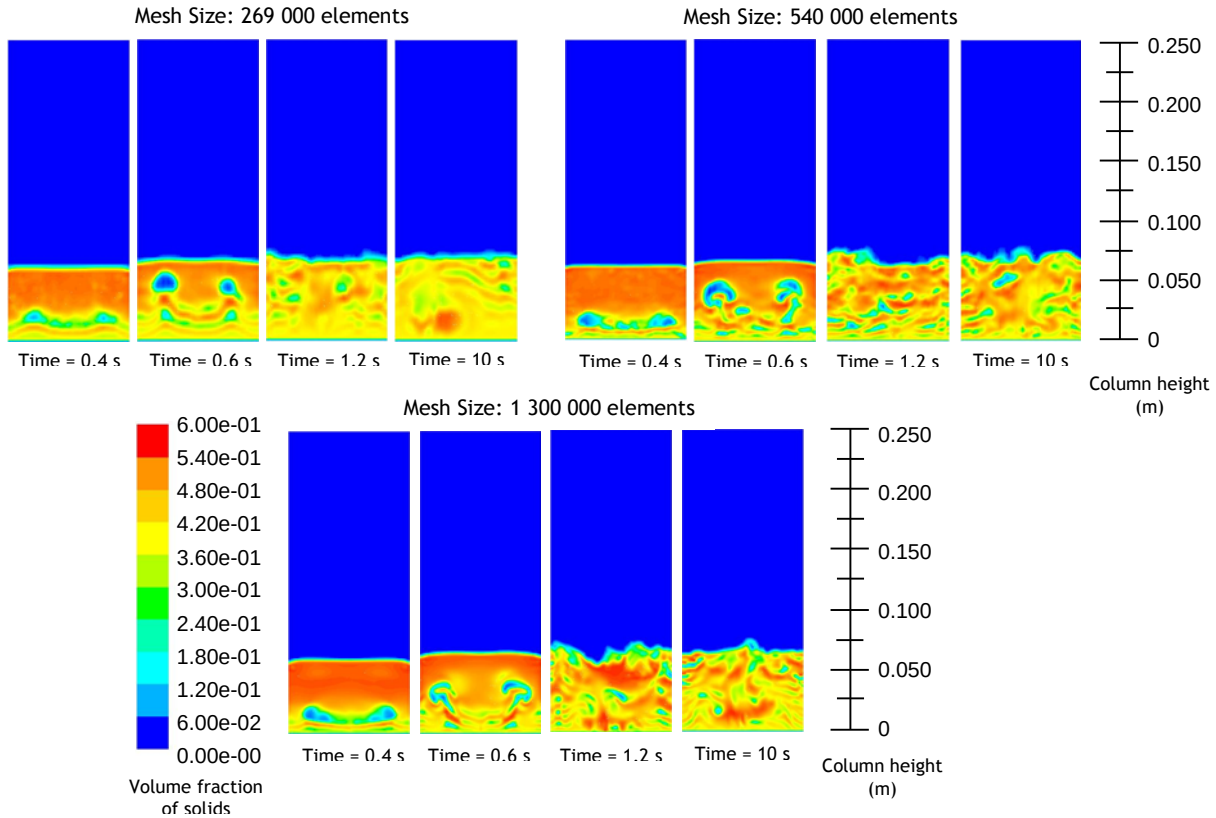

Figure 7. Dynamic sequence of the volume fraction of solids for 270k, 540k and 1 300k element grid at 0.4, 0.6, 1.2 and 10 s.

After analyzing Figure 7, it can be seen in the solutions that after a refinement equal to 540k elements there is no significant visual alterations. The numerical simulations for the 540k and 1 300k element grids predict an overall bed voidage around the value of 0.58 predicted by the Ergun equation for an inlet velocity of 0.065 m/s. The solids behavior remains constant after a certain number of elements in the mesh, so it can be concluded that the mesh with 540k elements (with a time step of 3.84×10^{-3} s) can provide mesh-independent results. Therefore, this mesh is used in the rest of simulations in this study.

5.1.3 Solid phase properties (settings)

Two different sets of properties for the solid phase were used to study their influence and are described in Table 2, one provided by a tutorial of a multiphase model example with heat transfer and with the Eulerian Granular method. The most prominent differences are in the methods used to model the granular viscosity, frictional viscosity and solids pressure.

In both simulations a column with 0.250 m of height and a mesh with 540 000 elements were used. The Figure 8 shows the overall bed voidage as function of time plot with the value obtained from the Ergun equation.

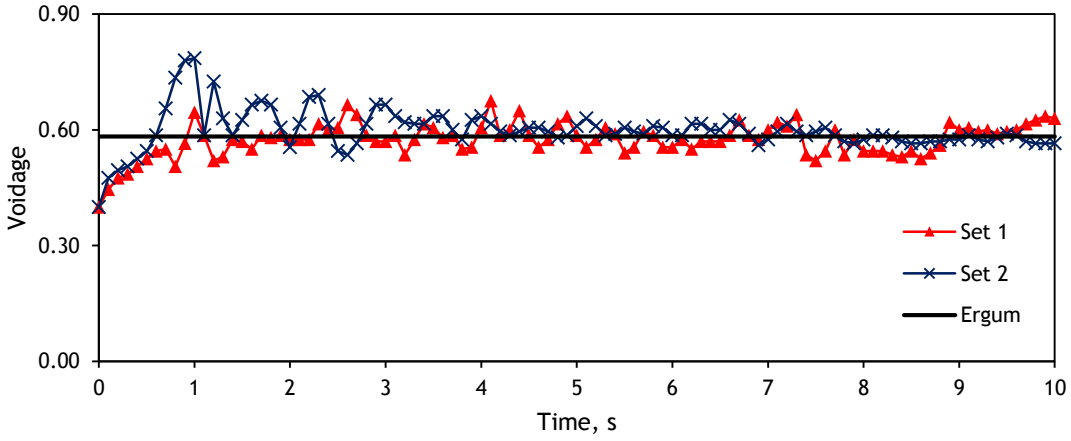

Figure 8. Effect of different set for the solid phase properties on overall voidage as a function of time.

Figure 8 shows two different particle behaviors: the simulation using the Set 1 of solid phase properties has small voidage fluctuations during the 10 s of flow time, while the simulation using the Set 2 has bigger fluctuations in the first 3 s, but they fade over time and have a more stable response. As this information is not enough to properly describe the phenomenon of the simulation using the second set of solid phase properties, the study of the solids movement (as volume fraction in Fluent®) is needed.

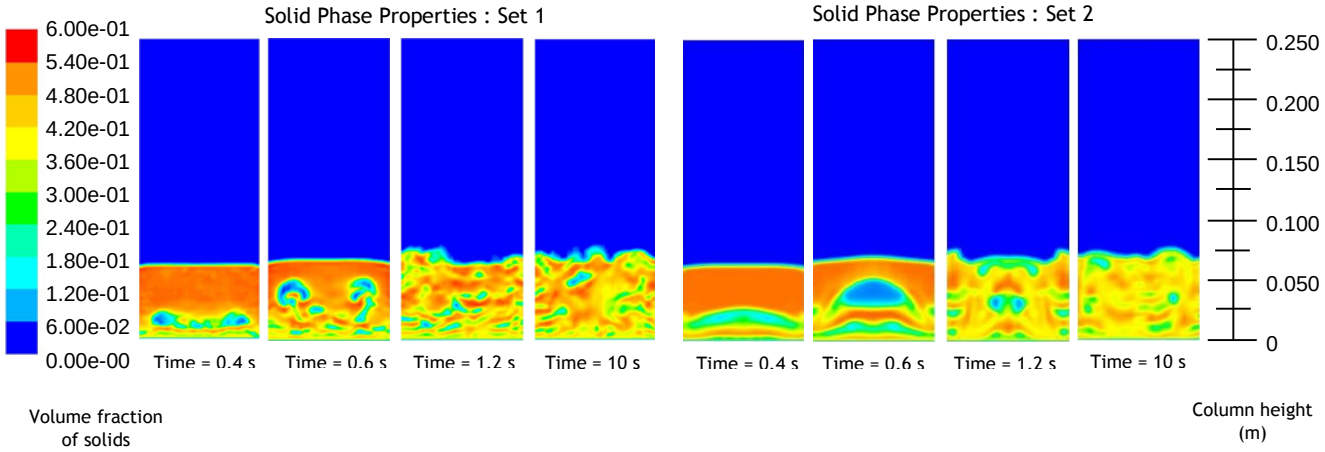

Figure 9. Dynamic sequence of the volume fraction of solids for the sets 1 and 2 simulations at 0.4, 0.6, 1.2 and 10 s.

In Figure 9, the evolution in time of the volume fraction of solids is shown for the settings suggested in the tutorial (left) and for the settings suggested in a training (right). In this figure, it can be noted that, when changing some methods to solve the properties for the solid phase, the particles behavior changes fundamentally.

In the simulation presented on the left (Set1), the bed particles, at the beginning of the flow, are dispersed and preferred paths are formed for the liquid flow. After a few moments, their behavior become unpredictable and random, creating zones with a higher volume fraction of solids. While in the simulation displayed on the right (Set 2), the first two snapshots at 0.4 and 0.6 s can explain the fluctuations in the overall voidage of the Figure 8, as it can be seen the formation of a large bubble. On the other hand, the particles motion starts to stabilize and there is a formation of a more homogeneous fluidized bed, as it is shown in the snapshot at 10 s. In section 5.2, further tests will be presented and validated, using data from the literature that will help to make a safe choice between these two sets.

5.2 Validation from experimental results

In this section, the developed Multi-Eulerian model is compared with experimental data from the work of Limtrakul *et al.* (2005). Limtrakul *et al.* (2005) worked with a column 0.14 × 1.5 m (diameter × height), which has a diameter comparable with the reactor in study (0.1 m). As proven in the preliminary studies, the column height has little influence in the simulation, so, even though the experimental column has a column height/diameter ration of 10, the column height is not considered very relevant. Three spherical particles with different materials and/or dimensions were studied by Limtrakul *et al.* (2005), wherein one of the trials spherical particles with ρ_s of 2500 kg.m^{-3} with 0.003 m of diameter have been used.

In Table 6 is presented the column characteristics from Limtrakul *et al.* (2005) and from this work. All the data obtained from Limtrakul *et al.* (2005) are from the column presented.

Table 6. Settings from the literature and this work.

	(Limtrakul et al. 2005)	This work
Column (diameter × height)	0.14 × 1.5 m	0.1 × 0.25 m
Particle diameter	0.003 m	0.003 m
ρ_s	2500 kg.m^{-3}	2500 kg.m^{-3}
Distributor	Perforated plate	Uniform inlet
Fluid	Tap water	Water
Voidage	0.44 (Dullien 1992)	0.4
Bed height	0.45 m	0.05 m

To validate the model, the axial velocities, the root mean square velocities and the azimuthally averaged solids holdup profiles from the simulations and the experimental data were compared.

The root mean square velocity (RMS vel.) is obtained from the Eq. 14 (Limtrakul *et al.*, 2005):

$$RMS = \sqrt{v'^2_k}, \text{ with } k = r, \theta, z \qquad \textit{Eq. 14}$$

where $v'_k = u_k - \overline{u_k}$. u_k is the instantaneous local velocity and $\overline{u_k}$ is the local time averaged velocity. To verify at what height the experimental data was provided, it was necessary to create three planes, in the axial direction, at 0.3, 0.4 and 0.5 m. In Figure 10, these planes and radial lines are defined.

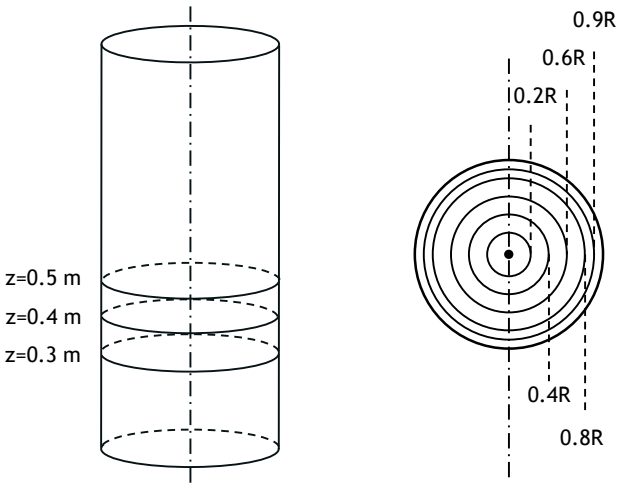

Figure 10. Planes and radial lines created for the voidage monitors

In Figure 11 shows the values obtained for the second plane, at 0.4 m high, which was the one with results closer to the experimental data. The results attained to the other two planes, 0.3 and 0.5 high, are shown in Appendix 2.

First, it was used the model with the Set 1 for solid phase properties and a no-slip condition at wall. After analyzing the results obtained for this simulation (Figure 11, top left/ red plot), it can be perceived that a no-slip condition doesn't describe the interaction between particles and wall.

Various tests were completed where it was studied different wall conditions: slip wall, and SC of 0.1, 0.3, and 1. In Figure 11 is shown the effect of these parameters on the axial velocity of the solids. While the top left and top right graphs use the Set 1 for the solid phase properties (studied in section 4.4) and the effect of slip condition and the SC are analyzed, respectively. The one in the bottom of Figure 11 uses the Set 2 of solid phase properties and analyzes the slip condition and a SC of 1.

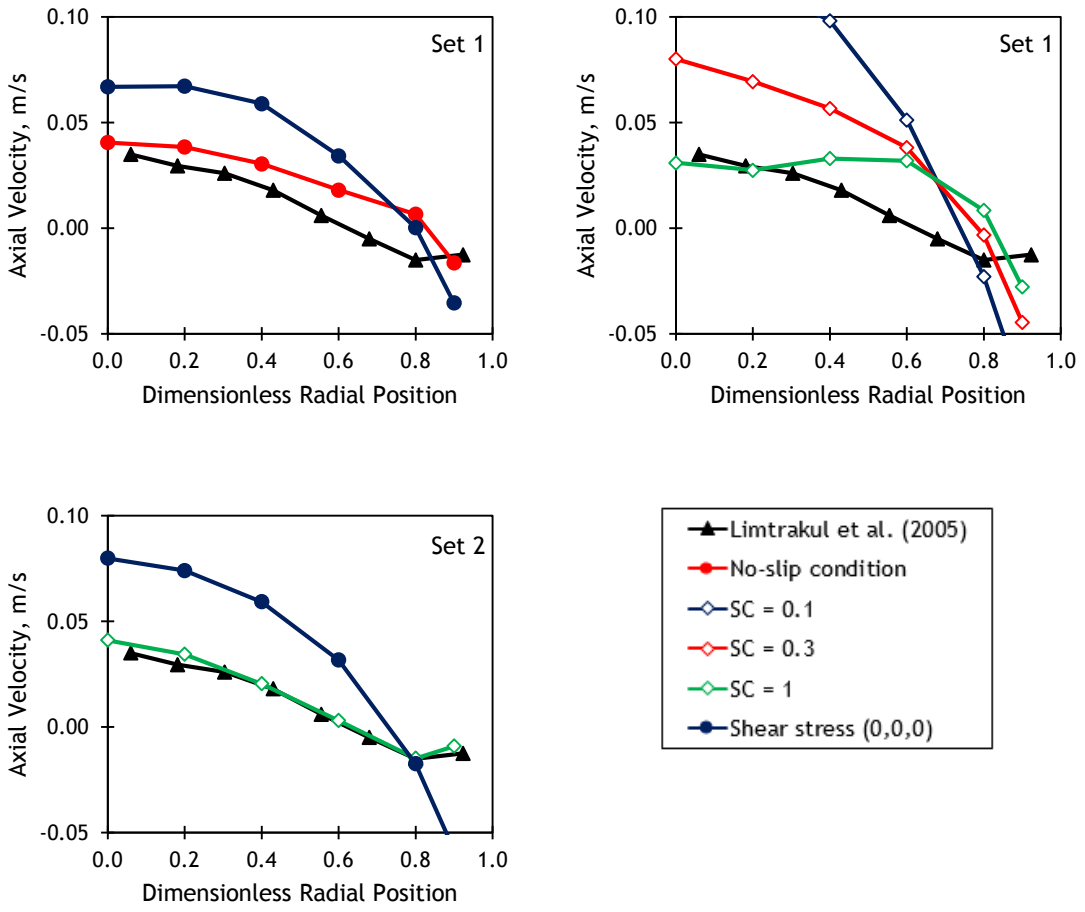

Figure 11. Effect of different parameters on the axial velocity in function of the dimensionless radial position (plane $z = 0.4$ m).

The simulation that better reproduces the experimental results is the one using the settings obtained from a training by Ansys® (Set 2) and specularity coefficient of 1, indicating that

there is a substantial amount of lateral collisions. As the column has a small diameter, there is a high probability for the particles to collide with the wall, so while in the simulation that uses a no-slip condition the results are not really that far from the experimental results, the condition does not describe accurately the particles behavior in the column. Regarding the effect of the SC, the increase of its value provides a behavior which is more alike to the experiments of Limtrakul *et al.* (2005). It can also be concluded that the Set 2 offers a better understanding of the real motion of a fluidized bed, something that it could not be established with the study in section 5.1.3. This result very satisfactory as it predicts accurately the mean axial velocities results of the literature, providing a validation for the developed model.

Figure 12 and Figure 13 show the evolution of the solids flow, evaluating different shear conditions at the wall at 0.5, 1, 2, 3, and 40 s.

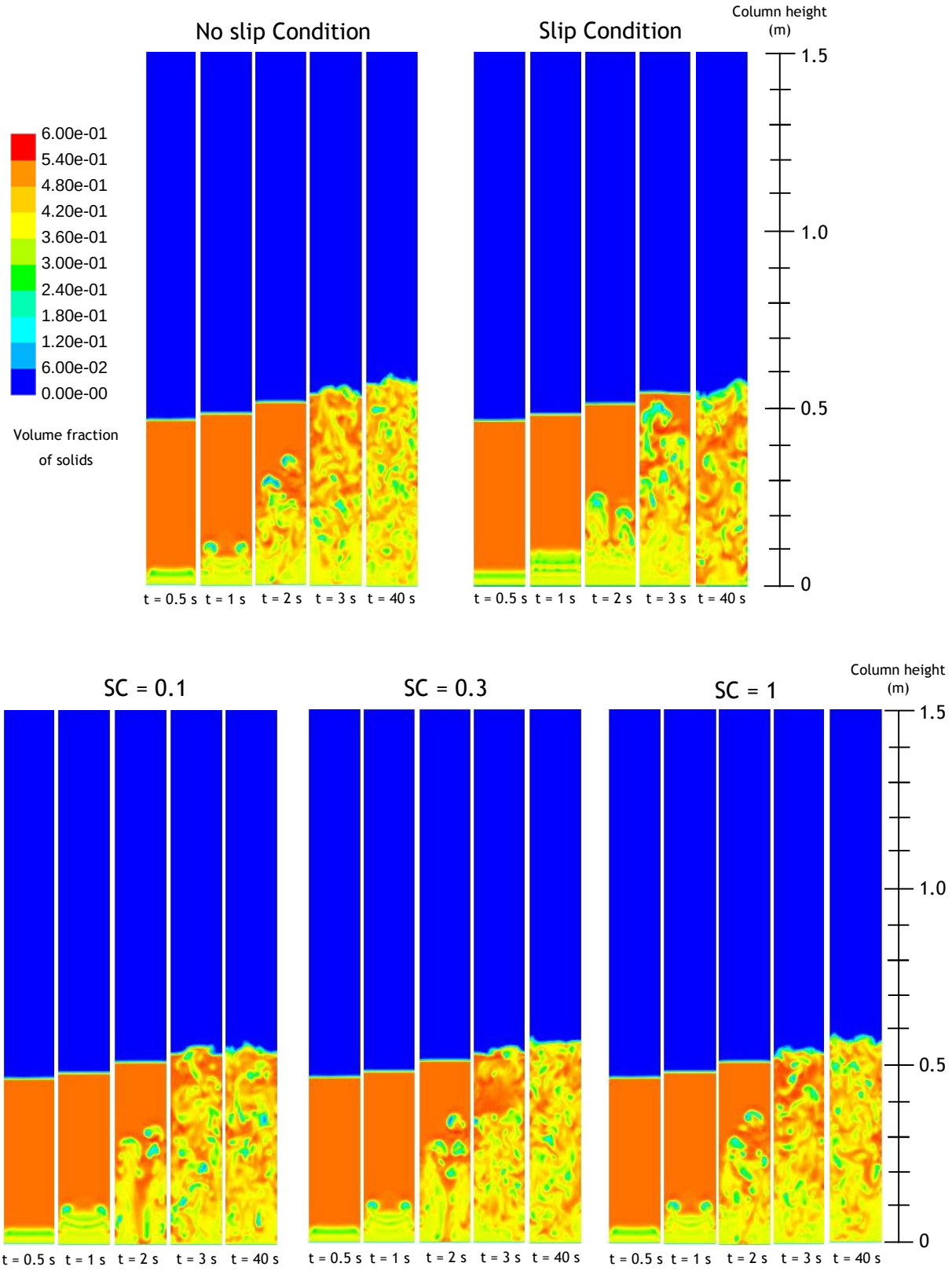

Figure 12. Dynamic sequence of the volume fraction of solids for the slip condition, no-slip condition, and SC of 0.1, 0.3, and 1 at 0.5, 1, 2, 3 and 40 s, using the Set 1.

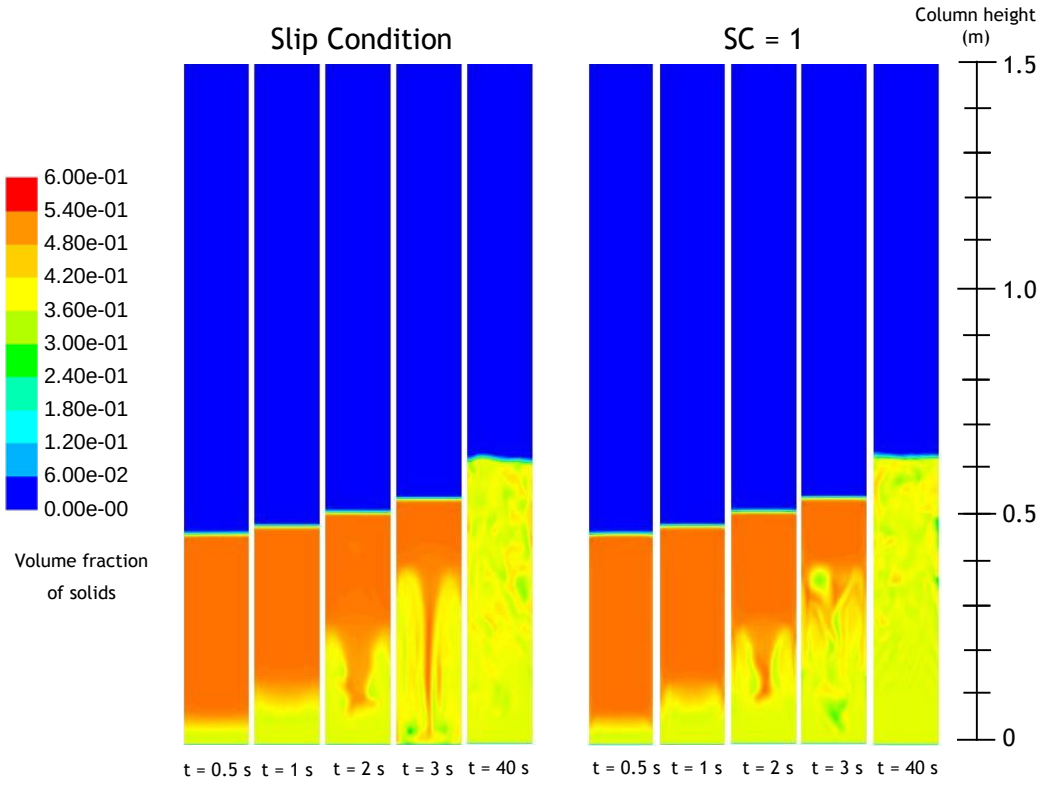

Figure 13. Dynamic sequence of the volume fraction of solids for the slip condition and SC of 1 at 0.5, 1, 2, 3 and 40 s, using the Set 2.

After analyzing both Figure 12 and Figure 13, it can be seen in the solutions that the simulation using the second set of solid phase properties and the specularity provide the more stable and homogeneous behavior. In Figure 12, the first two dynamic sequences compare the slip condition, and it can be seen that the solids behavior is irregular, but different in each simulation, as the simulation with the no-slip condition at the wall has a bigger homogenous zone. The last three dynamic sequences presented in this figure, compare the influence of the specularity coefficient. As it can be seen, in the first seconds, the particulate medium behaves similarly. However, when the solids stabilize (40 s), the homogeneity of the medium increases with the increasing of the SC.

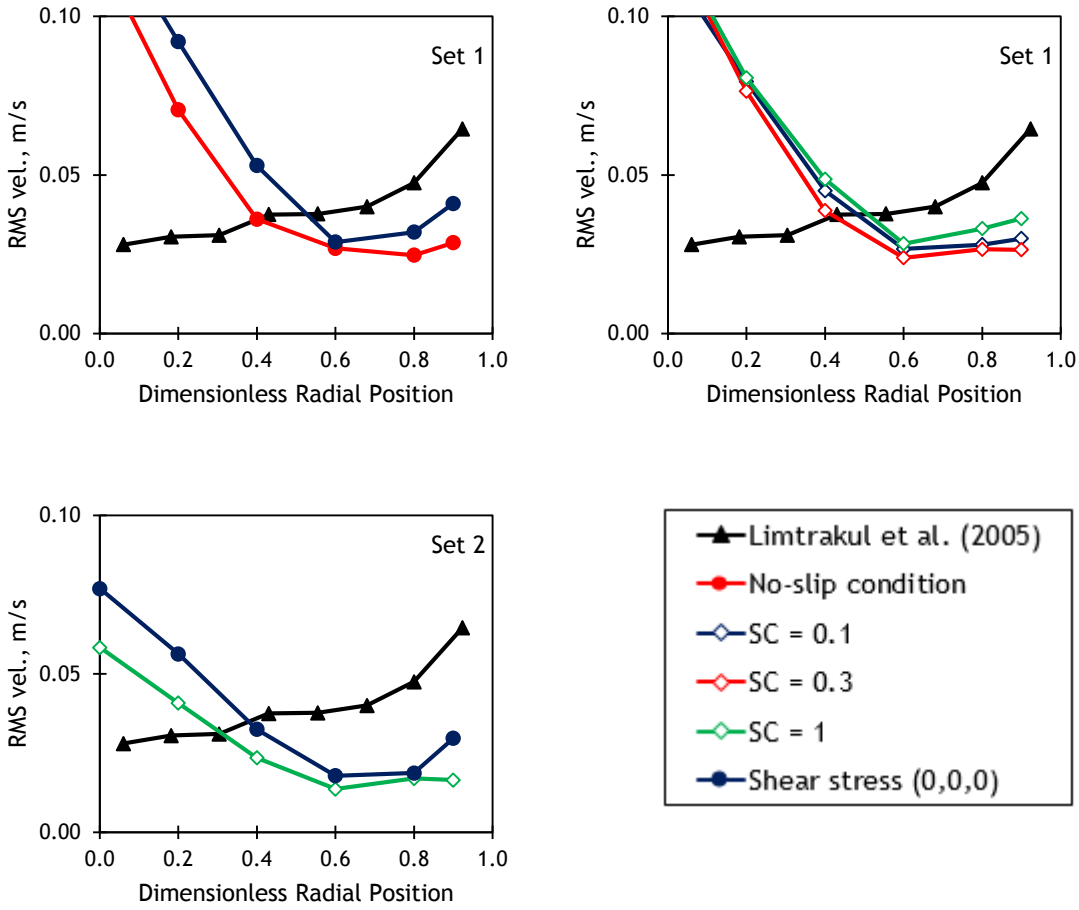

Figure 14. Effect of different parameters on the RMS velocity in function of the dimensionless radial position (plane z=0.4 m).

Figure 14 shows all the obtained RMS velocities obtained for the simulations. The more notorious difference that can be visualized is between the results while using the Set 1 or Set 2 for the solid phase properties. Even though none the results attained with the CFD simulations describe the experimental data from (Limtrakul *et al.*, 2005), only the two simulations using the second set of properties, are within the same order of magnitude of the experimental values. More studies have to be made to have a better understanding of what influences the fluctuations in the axial velocity to behave like that, as a laminar regime to describe the flow is used. Future studies with a turbulent regime will have to be carried out, to verify the influence on the velocity fluctuations.

In Figure 15 is shown the overall solids holdup for the simulation using the second set of solid phase properties and a specularity coefficient of 1.

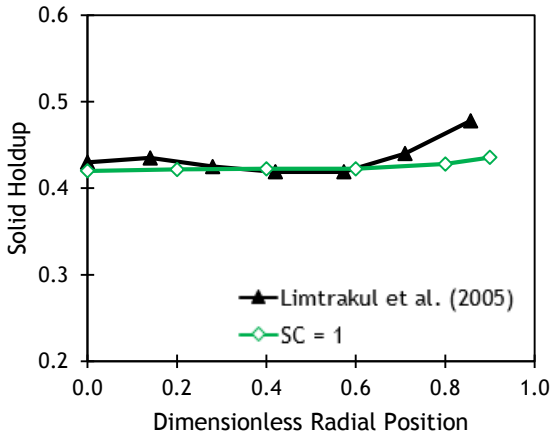

Figure 15. Overall solids holdup as a function of the dimensionless radial position (simulation using Set 2 and SC of 1).

It can be seen in Figure 15 that the overall solids holdup for the simulation using the second settings of solid phase properties and a SC of 1 are around the overall solids holdup obtained from the literature. The literature results show a fraction of solids of 0.43 in the middle of the column and of 0.48 closer to the wall, while the results obtained from the simulation are between 0.43 and 0.44. These results are very satisfactory and sustain the validation of the model.

6 Conclusion

A simpler model of a liquid-solid ebullated bed reactor with spherical particles was explored. The developed model was validated by comparing the simulation results with a similar case study available in the literature.

The Euler-Euler multiphase modeling approach was used to simulate fluid flow through an originally settled bed, until a perfectly fluidized state is reached. Several preliminary studies were completed and showing that the column height does not influence substantially the simulation results. However the grid sensibility study has a higher impact on the bed behavior. The grid with 540k elements (Δx of 2.5×10^{-3} m and 200 axial divisions) provides mesh-independent. The study of the solid phase properties was more difficult to analyze, and even though the two settings described different particle bed behaviors, both tended to the same voidage value.

The CFD model was validated according to the literature results found and the particle-wall collisions were described by a specularity coefficient of 1, while using the Set 2 of solid phase properties. When comparing the mean axial velocity results between the model and the literature, we can conclude that they were well predicted. However, there is still work to be done in this model to predict the radial distribution of the velocity fluctuations.

Moreover, the study case provided valuable information to choose between the two settings, as the behavior of the second set is much more realistic with a higher particle bed.

This work allowed to define different simulation parameters suitable for this model. Among all the simulations performed, the mesh with the length of 0.25 m and 540k elements, using the Set 2 and a specularity coefficient of 1 to describe the characteristics of the solid phase and the interaction between the particles and the reactor wall, respectively, provides better experimental results.

6.1 Limitations and Future Work

Numerical tools and CFD models are showing to be very useful for preliminary studies of processes. However, the use of these tools force building the model along with the geometric mesh, which reduce the available time of the development phase. Moreover, the literature is still lacking information about the different parameters to characterize and validate the models.

The present work offers understanding on fluidized liquid-solid flow on ebullated bed reactors. Nevertheless, no studies on a tree-phasic (gas-liquid-solid) and cylindrical particle reactor were yet executed. Since the objective, besides serving as a base case for further

works on liquid-solid fluidized beds, was to describe the ebullated reactor at pilot scale, the following future work can be suggested:

- The application of the validated model, with new proper considerations, to a three-phasic reactor and confirm the model with experimental data from the literature (e.g., Fraguío *et al.*, 2007; Jin, 2006).
- The validation of the model for a liquid-solid ebullated bed using cylindrical particles instead of spherical particles.
- The introduction of an adapted inlet velocity profile to describe the flow produced by a propeller and analyze the effect on the overall voidage.

Overall, even with some limitations, CFD modeling is showing to be an interesting tool to study fluids behavior in deeper detail, and also to study heat and mass transfer in ebullated bed reactors.

6.2 Final Appreciation

It was extremely rewarding to work in this project, since the knowledge obtained from the different fields and people permitted me to acquire new concepts that surely will be useful in the future. Mainly, the understanding of the possibilities and limitations of Computational Fluid Dynamics models helped to learn new tactics to solve Chemical Engineering problems. Overall, this opportunity was a very gratifying professional experience.

7 References

Chaouki, J.; Larachi, F.; Duduković, M. P. (1997) Non-invasive monitoring of multiphase flows. Amsterdam, New York: Elsevier.

Chen, R. C.; Reese, J.; Fan, L.-S. (1994) Flow structure in a three-dimensional bubble column and three-phase fluidized bed. In: AIChE Journal, vol. 40, n° 7, p. 1093–1104. DOI: 10.1002/aic.690400702.

Cornelissen, J. T.; Taghipour, F.; Escudié, R.; Ellis, N.; Grace, J. R. (2007) CFD modelling of a liquid–solid fluidized bed. In: Chemical Engineering Science, vol. 62, n° 22, p. 6334–6348. DOI: 10.1016/j.ces.2007.07.014.

Dadashi, A.; Zhu, J.; Zhang, C. (2014) A computational fluid dynamics study on the flow field in a liquid–solid circulating fluidized bed riser. In: Powder Technology, vol. 260, p. 52–58. DOI: 10.1016/j.powtec.2014.03.030.

Del Bianco, A.; Panariti, N.; Di Carlo, S.; Beltrame, P. L.; Carniti, P. (1994) New Developments in Deep Hydroconversion of Heavy Oil Residues with Dispersed Catalysts. 2. Kinetic Aspects of Reaction. In: Energy & Fuels, vol. 8, n° 3, p. 593–597. DOI: 10.1021/ef00045a013.

Dullien, F. A. L. (1992) Porous Media Fluid Transport and Pore Structure. 2nd Revised edition: Academic Press Inc.

Ergun, Sabri (1952) Fluid Flow through Packed Columns. In: Chemical Engineering Progress, vol. 48, 1952, p. 89–94.

Fraguío, María Sol; Cassanello, Miryan C.; Larachi, Faïçal; Limtrakul, Sunun; Dudukovic, Milorad (2007) Classifying flow regimes in three-phase fluidized beds from CARPT experiments. In: Chemical Engineering Science, vol. 62, n° 24, p. 7523–7529. DOI: 10.1016/j.ces.2007.08.039.

Garside, J.; Al-Dibouni, M.R. (1977) Velocity-Voidage Relationship for Fluidization and Sedimentation in Solid–Liquid Systems. In: Ind. Eng. Chem. Precess Des. Dev., vol. 16, 1977, p. 206–214.

Gidaspow, W. (1994) Multiphase Flow and Fluidization-Continuum and Kinetic Theory Descriptions. In: Academic Press, 1994.

Jin, Guodong (2006) Multi-scale modeling of gas–liquid–solid three-phase fluidized beds using the EMMS method. In: Chemical Engineering Journal, vol. 117, n° 1, p. 1–11. DOI: 10.1016/j.cej.2005.12.009.

Kiared, K.; Larachi, F.; Cassanello, M.; Chaouki, J. (1997) Flow Structure of the Solids in a Three-Dimensional Liquid. In: Industrial & Engineering Chemistry Research, p. 4695–4704.

Larachi, F.; Cassanello, M.; Chaouki, J.; Guy, C. (1996) Flow structure of the solids in a 3-D gas–liquid–solid fluidized bed. In: AIChE Journal, vol. 42, n° 9, p. 2439–2452. DOI: 10.1002/aic.690420905.

Limtrakul, Sunun; Chen, Jinwen; Ramachandran, Palghat A.; Duduković, Milorad P. (2005) Solids motion and holdup profiles in liquid fluidized beds. In: Chemical Engineering Science, vol. 60, n° 7, p. 1889–1900. DOI: 10.1016/j.ces.2004.11.026.

Richardson, J.F.; Zaki, W.N. (1954) Sedimentation and fluidisation: Part I. In: Trans. Inst. Chem. Eng., vol. 32, 1954.

S. Kressmann, C. Boyer, J.J. Colyar, J.M. Schweitzer and J.C. Viguié (2000) Improvements of Ebullated-Bed Technology for Upgrading Heavy Oils. In: Oil & Gas Science and Technology, vol. 55, n° 4, p. 397–406.

Zhu, Jesse; Leckner, Bo; Cheng, Yi; Grace, John (2005) Multiphase Flow Handbook. Fluidized Beds. : CRC Press.

Appendix 1 – Grids

In Figure 16 is show the grids used in the grid sensibility study, the lateral and top/bottom views. The grid in the left corresponds to the one with 270 000 elements; the one in the center has the same structure, in the top/bottom view of the column, as the one on the left, nonetheless, it has more divisions in the lateral view, corresponding to the grid with 540 000 elements; and the one in the right is the most refined mesh from the presented (1 300 000 elements), and it can be visualized the four divisions made to maintain the skewness reduced.

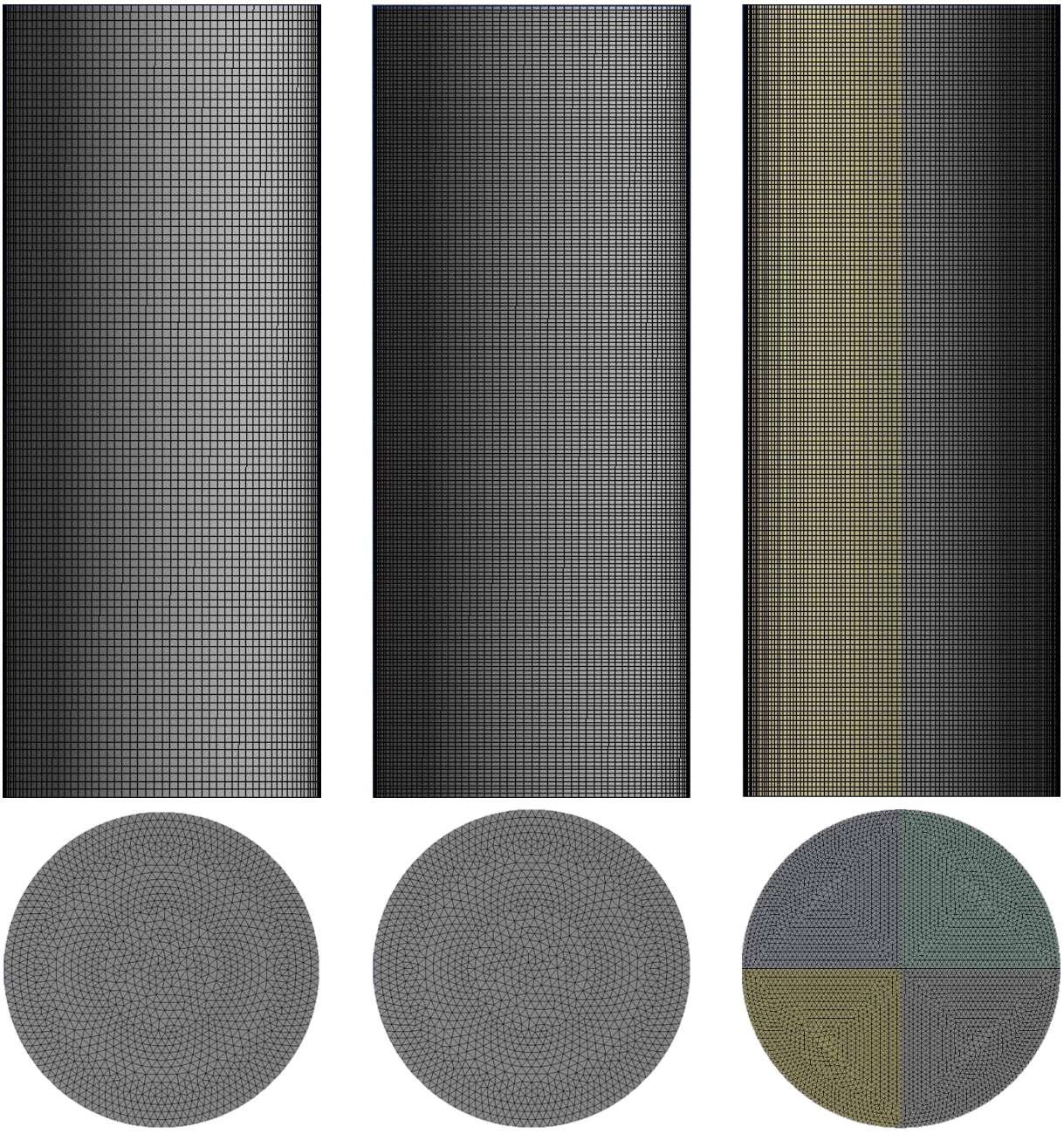

Figure 16. Lateral and top/bottom views from the 240k, 540k, and 1 300k element grids.

Appendix 2 - Effect of the shear conditions at the wall on the axial velocity

In Figure 17 and Figure 18 show the values of the solids mean axial velocity obtained for the first plane, at 0.3 m high, and for the third plane, at 0.5 m high, respectively.

Different wall conditions were studied: slip wall, and SC of 0.1, 0.3, and 1. In the top left graph, it is analyzed the effect of slip condition and is used the Set 1 for the solid phase properties (studied in section 4.4). The top right graph analyzes the effect of the specularity coefficient, and it is also used the Set 1. In bottom graph, settings obtained from a training by Ansys® (Set 2) is used in the simulations and it was studied the slip condition and a SC of 1.

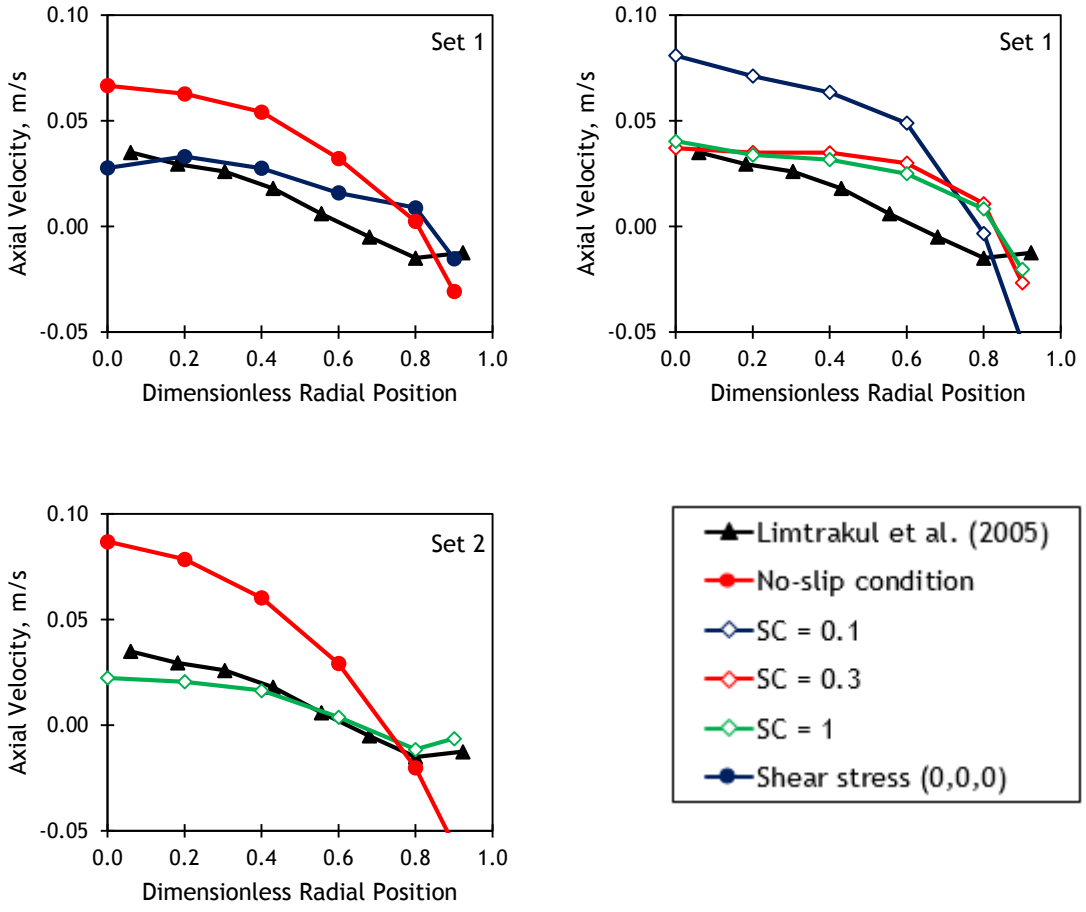

Figure 17. Effect of different parameters on the axial velocity in function of the dimensionless radial position (plane $z = 0.3$ m).

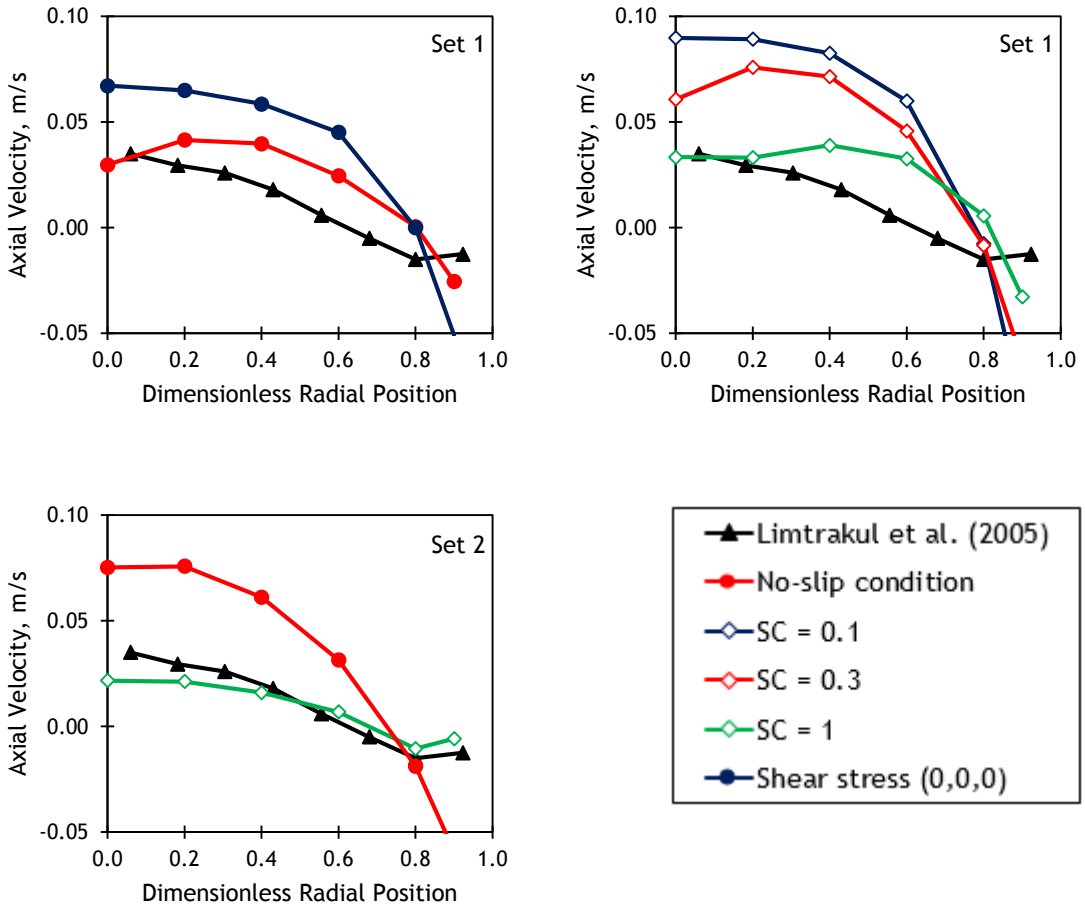

Figure 18. Effect of different parameters on the axial velocity in function of the dimensionless radial position (plane $z = 0.5$ m).

Even though the results for the second plane, at 0.4 m high, are closer to the experimental data, in Figure 17 and Figure 18 can also be seen that the simulation using the Set 2 and a SC of 1 is the simulation that better reproduces the results from the literature.

The Figure 19 and Figure 20 show all the obtained RMS velocities obtained for the simulations, in the first and third plane. As discussed in section 5.2, none the results attained with the CFD simulations describe the experimental data from Limtrakul *et al.* (2005). However, it can be seen a difference between the results while using the Set 1 or Set 2 for the solid phase properties, as only the two simulations, using the second set of properties, are of the same order as the experimental values.

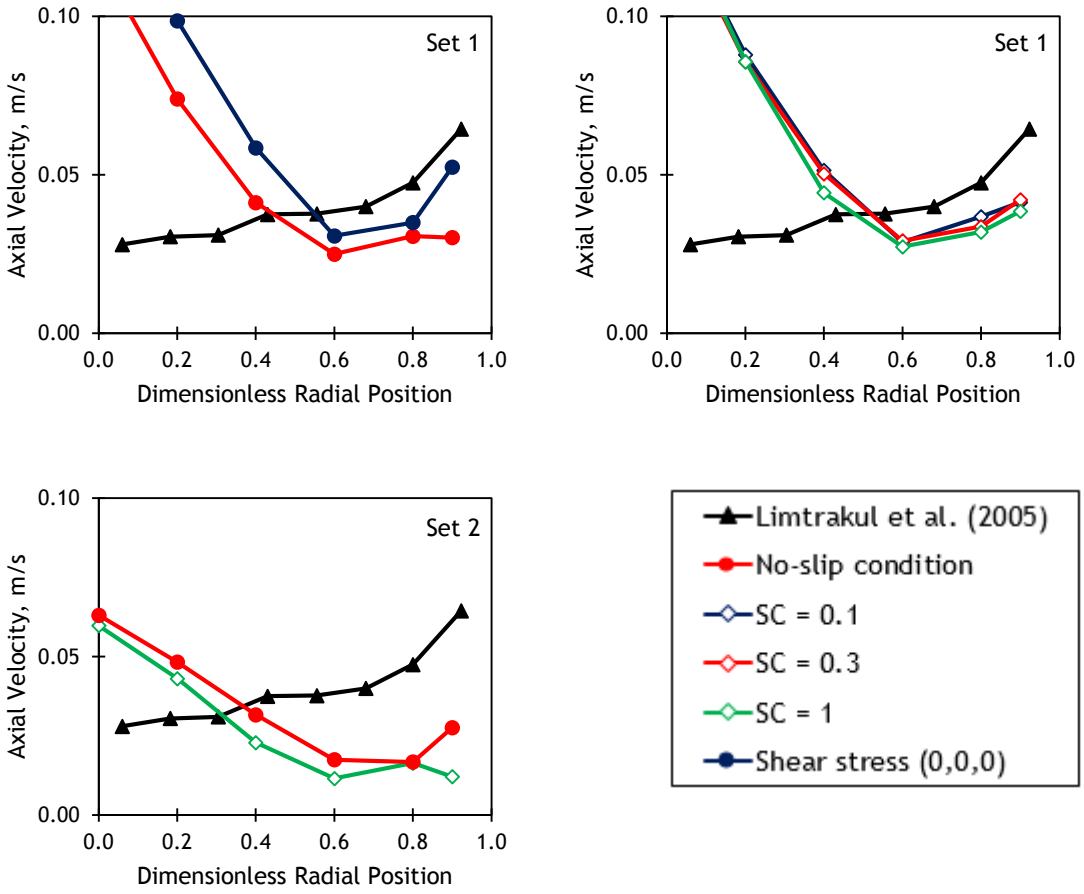

Figure 19. Effect of different parameters on the RMS velocity in function of the dimensionless radial position (plane $z = 0.3$ m).

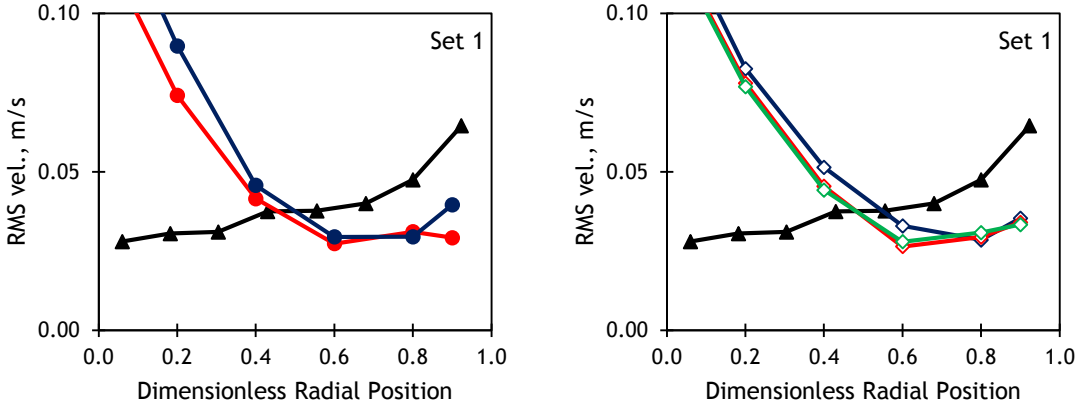

Figure 20. Effect of different parameters on the RMS velocity in function of the dimensionless radial position (plane z=0.5 m) (cont.).

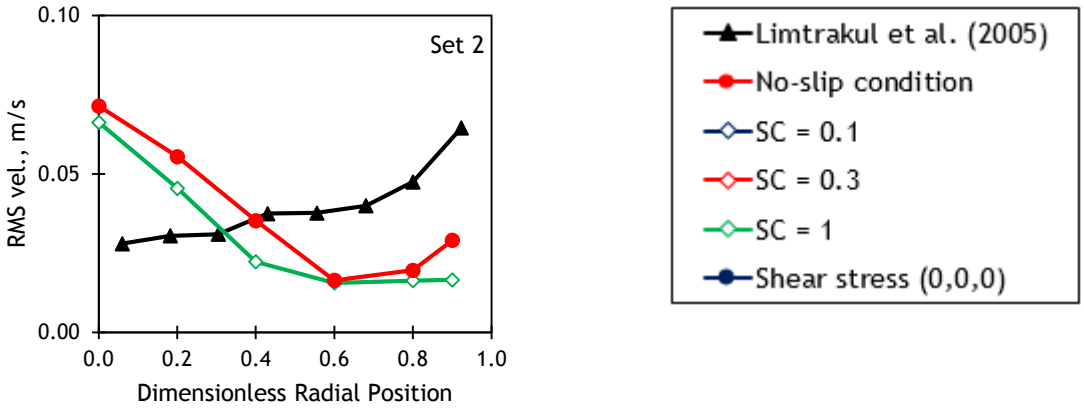

Figure 21. Effect of different parameters on the RMS velocity in function of the dimensionless radial position (plane z=0.5 m) (cont.).